Peak Cancellation scheme for OFDM Signals with Performance Analysis

M.VIJAY KRISHNA & D.V.S.R SESIDHAR
Assistant professors, Dept. of ECE, M.V.S.R ENGINEERING COLLEGE, NADERGUL, RANGAREDDY, TELANGANA, INDIA

Received: May 02, 2018 Accepted: June 11, 2018

ABSTRACT *Peak cancellation (PC) is known as one of the simplest peak-to-average power ratio (PAPR) reduction techniques that are applicable to various communications standards. The salient advantage of PC is its ease of hardware implementation, but it induces in-band distortion and out-of-band distortion. In order to restrict the amount of distortion within an acceptable level, it is critical to carefully design the cancelling pulses as well as the envelope threshold over which PC is applied. In most studies, however, they are determined empirically through computer simulations. This paper thus focuses on a rigorous theoretical analysis of PC applied to band-limited orthogonal frequency division multiplexing (OFDM) signals, and discusses its validity and limitation for practical applications. Based on the level-crossing rate approximation of the peak distribution, we derive a closed-form expression for the achievable signal-to-distortion power ratio (SDR). We also analyze the adjacent channel leakage ratio (ACLR) as well as error vector magnitude (EVM), with which the symbol error rate (SER) over an additive white Gaussian noise (AWGN) channel is obtained. All the theoretical results developed in this work are compared with those based on the corresponding computer simulations to justify our analytical approach. It thus serves as a useful and accurate tool for designing cancelling pulses as well as the threshold level, for given specific system requirements such as SDR (or EVM) and ACLR.*

Keywords: *Adjacent channel leakage ratio (ACLR), error vector magnitude (EVM), orthogonal frequency division multiplexing (OFDM), peak cancellation (PC), peak-to-average power ratio (PAPR), signal-to-distortion power ratio (SDR), symbol error rate (SER).*

I. INTRODUCTION

Recently, there has been much interest in using multicarrier modulation in a wide variety of application scenarios [1].The most well-known ones are DMT (Discrete Multitone) in the wired ADSL (asymmetric digital subscriber line) and VDSL (very high-rate digital subscriber line) domain [2], and OFDM, or orthogonal frequency division multiplexing, for a variety of wireless applications such as DAB (digital audio broadcasting), DVBT (digital video broadcasting- terrestrial), Wireless LANs, MANs, and high-speed cellular data [3]. In all these systems, information is transmitted in parallel on several, orthogonal subcarriers, each subcarrier being QAM/ PSK modulated. As the number of subcarriers N becomes large, the multicarrier (OFDM) baseband signal can be quite accurately represented as a complex Gaussian process with Rayleigh envelope distribution and uniform phase distribution [4],[5]. The Gaussian approximation is a consequence of the Central Limit Theorem and is very realistic for most practical systems ($N \geq 64$) of interest.

Considerable attention has recently been given to the application of statistical methods to communication problems. Some of these problems involve stationary random noise signals possessing gaussian distributions of amplitudes. It is sometimes desirable to determine the autocorrelation and cross correlation functions of such signals after they undergo nonlinear amplitude distortion in terms of the original correlation functions. Analysis based on the ergodic hypothesis and on some well-known properties of the gaussian variable can be applied. It is the purpose of this report to present some of the results of this analysis which do not seem to have been noted yet in the literature and to indicate where they may be found useful. We begin by outlining the technique of correlation analysis of distorted gaussian signals.

Due to the nonlinear nature of many analog devices, the actual analog front-end that should operate with a large linear range entails significant cost and power loss. Therefore, extensive research has been conducted focusing on achieving low PAPR in the digital front-end.

The digital front-end is an intermediate between the physical layer and analog devices, and it primarily serves for frequency shifting, resampling, filtering, and impairment compensation for the analog front-end [6]. The PAPR reduction carried out in the digital front-end gives no change to the physical layer and thus is commonly applied in practice. Provided that the resulting error vector magnitude (EVM) is tolerable, PAPR can be reduced to a certain level by introducing some degree of distortion. Meanwhile, the signal after PAPR reduction should conform to the spectral mask. More specifically, the adjacent channel leakage ratio (ACLR) should meet the system requirement [7].

Among many PAPR reduction techniques, most of the so called distortion-less approaches (such as selective mapping [8]) is not applicable to the standardized OFDM systems as they call for major modifications in the physical layer architecture. This paper thus focuses on the techniques that are standard-compliant, and such approaches include clipping and filtering (CAF) [9], [10] and peak cancellation (PC) [11].

Orthogonal Frequency Division Multiplexing (OFDM) is an navigating technology for 3G and 4G Wireless and Mobile communication. OFDM is multiplexer and multicarrier technology disburses the data over large number of carriers spaced at definite frequencies. The interval provides orthogonality. OFDM is operated in wired coaxial line i.e., xDSL cables and wireless communication like DVB, DAB, IEEE802.11, IEEE802.20, Wi-Fi, Wi-Max. OFDM is a multicarrier which suppresses multipath distortion and improves spectral efficiency. Due to orthogonal carriers, OFDM signal has high PAPR which lowers efficiency of HPA. The high PAPR is mitigated by many techniques like clipping, peak windowing, peak cancellation, companding, tone reservation, tone injection or by distorting the signal or by scrambling and spreading the signal like selected mapping(SLM), partial transmit sequence(PTS), interleaving, precoding by using liable sequences.

In principle, CAF induces peak re growth due to the existence of the post-clipping filter to meet the spectral constraint, resulting in intractable PAPR re growth. On the other hand, PC does not cause any PAPR re growth but does exhibit out-of-band distortion caused by the cancelling pulse. By judicious design of peak cancelling pulses, however, the PAPR can be reduced while the out-of-band distortion is kept negligible. Moreover, since there is no need to invoke an additional filter (which contains a number of multipliers) for the out-of-band suppression, PC has lower complexity than CAF when implemented by hardware [13], [12]. Our companion paper [13] demonstrates a low-complexity real-time implementation of PC techniques using FPGA. Applications of the PC concept to other PAPR reduction techniques such as active constellation extension and tone reservation, and their design issues have been addressed in, e.g., [14] and [15].

Performance analysis of deliberately clipped OFDM signals can be found in, e.g., [9], [16], [17] and similarly the OFDM system after nonlinear power amplification is theoretically analyzed in, e.g., [18], [19]. Nevertheless, attempts for theoretical analysis of the OFDM system with PC are rather scarce. A bit error rate analysis of PC is found in [20], but it fails to address the resulting power spectrum, an important factor upon designing peak cancelling pulses under a given ACLR constraint. The difficulty in rigorous spectral analysis of PC stems from the fact that the PC event is a point process and thus it cannot be explicitly modeled by a stationary process.

In this paper, we theoretically analyze the performance of an OFDM system operated with PC. Provided that the baseband OFDM signal is characterized as a band-limited complex Gaussian process, a closed-form expression of signal to-distortion power ratio (SDR) is firstly derived based on the level-crossing rate approximation of the peak distribution. Furthermore, by analyzing a cancelling pulse function, ACLR and EVM of the OFDM signal after PC are calculated. These results allow us to theoretically determine the threshold level that can meet the distortion requirement (in terms of SDR, EVM, and ACLR). The obtained results are then used for deriving the symbol error ratio (SER) of the OFDM system with M-ary quadrature amplitude modulation (M-QAM), transmitted over an additive white Gaussian noise (AWGN) channel in the presence of PC. The accuracies of all the theoretical results developed here are confirmed by the corresponding simulations.

The remainder of this paper is organized as follows. Section II describes the OFDM transmission system and the generic PC model adopted in this paper. Our analytical framework of SDR derivation based on the level-crossing rate approximation is developed in Section III. Section IV carries out the derivation of the distortion caused by PC in frequency domain, based on which the resulting ACLR and EVM are theoretically analyzed. Considering the scenario of transmitting the peak cancelled signal over an AWGN channel, theoretical expressions of SER performance are also derived. The amount of distortion based on the theoretical analysis is verified through computer simulations in Section V. Finally, conclusions are given in Section VI.

II. SYSTEM DESCRIPTION

In this section, we briefly review a commonly adopted description of the OFDM signal and then introduce the PC system considered in this paper. A. OFDM Signal Formulation Let A {A0, A1..., AN−1} denote the data sequence to be transmitted by one OFDM symbol with N subcarriers, where A_k represents the complex data of the kth subcarrier. The complex baseband OFDM symbol can be expressed as

$$s(t) = e^{j\phi_t} \frac{1}{\sqrt{N}} \sum_{k=0}^{N-1} A_k e^{\frac{j2\pi kt}{T_s}}, \quad 0 \le t < T_s, \qquad (1)$$

Where Ts is one OFDM symbol period without guard interval. Hence the Nyquist interval T of the N-subcarrier OFDM symbol can be defined as T = Ts/N. The frequency offset φt introduced in (1) is given by [6]

$$\phi_t = \frac{t(1-N)}{T_s}\pi. \qquad (2)$$

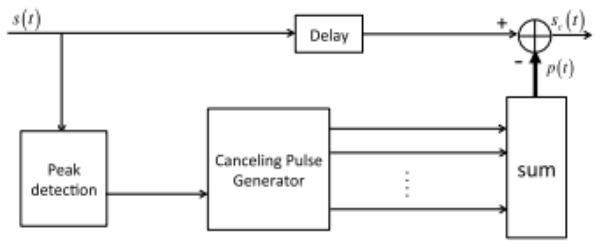

Fig.1. A block diagram of PC procedure in hardware implementation [10].

Let s (t) = x (t) + j y(t), where x(t) and y(t) are the real and imaginary parts of s(t), respectively. Assume that x (t) and y (t) are statistically independent Gaussian random processes and that they are band-limited and stationary with zero mean [2]. Without loss of generality, their variances are set such that

$$E\left\{|x(t)|^2\right\} = E\left\{|y(t)|^2\right\} = \frac{1}{2}, \qquad (3)$$

Where E {·} denotes an expectation. It then follows that s(t) is a stationary complex Gaussian random process with zero mean and unit variance, i.e., we have E{s(t)} = 0 and E{|s(t)| 2} = 1 for any time instant t. The corresponding envelope r (t) = x2 (t) + y2 (t) is a random process that follows Rayleigh distribution. The pdf of r(t) is thus given by

$$f_r(r) = 2re^{-r^2}. \qquad (4)$$

B. Peak Cancellation Model

The principle of PC is to generate cancelling pulses at the time instances where the peaks higher than the predetermined threshold γ are found and to subtract them from the original signal. An example block diagram suitable for practical implementation [10] is depicted in Fig. 1. In what follows, we denote the polar expression of the OFDM signal by s(t) = r(t)e jθ (t) , where r(t) and θ (t) represent the envelope and phase of the original signal s(t), respectively. Suppose that there are Nρ(γ) peaks that are higher than the threshold γ in the envelope process r(t) during one OFDM symbol interval, and let ti denote the time instant at which the ith peak is observed, where i ∈ {1, 2,..., Nρ(γ)}. The signal after peak cancellation can then be written as

$$s_c(t) = s(t) - \underbrace{\sum_{i=1}^{N_\rho(\gamma)} p_i(t - t_i)}_{p(t)}, \qquad (5)$$

Where pi(t) denotes the cancelling pulse corresponding to the ith peak with an appropriate time shift such that pi(t) has a peak at t = 0, and p(t) is the sum of all the cancelling pulses generated within one OFDM symbol. In this work, we express the ith cancelling pulse in the following form [10]

$$p_i(t) = (\rho_i - \gamma)\, e^{j\theta_i}\, g(t), \qquad (6)$$

Where ρi = r (ti), θ_i = θ (ti), and g (t) is a dedicated impulse response function referred to as a cancelling pulse kernel in what follows. Example waveforms corresponding to s(t), sc(t), and p(t) are plotted in Fig. 2. Note that if the fluctuation of average power due to the subtraction of the cancelling pulses is negligible, the square of the threshold γ serves as a strict PAPR that can be achieved by the PC system.

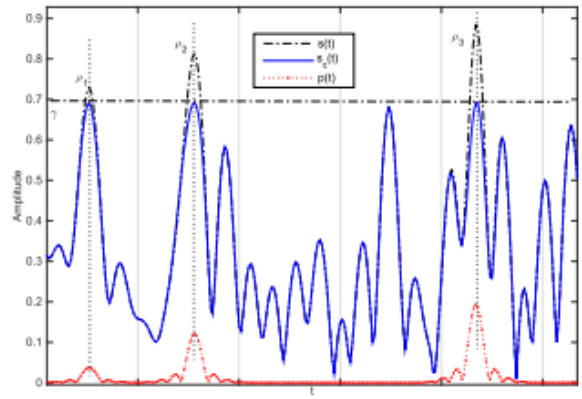

Fig.2. Example waveforms associated with PC where ρi denotes the envelope level of the ith peak.

Therefore, we alternatively refer to γ as the target PAPR in what follows. By observing (6), one can find that the distortion caused by PC depends on g(t) as well as the target PAPR γ , and this issue will be discussed in Section IV.

III. SIGNAL-TO-DISTORTION POWER RATIO ANALYSIS OF PEAK CANCELLATION FOR OFDM SIGNALS

Assuming that the OFDM signal is approximated by a complex Gaussian random process, the standard approach for statistical characterization of the signal after nonlinear processing is the use of Buss gang's theorem [21], [22]. We model the OFDM signal after PC as a linear transform of the input signal and additive distortion given by [23]

$$s_c(t) = \alpha_\gamma s(t) + d(t), \qquad (7)$$

Where d (t) is the distortion term and αγ is a constant attenuation factor that depends on the threshold γ . The input process s (t) is uncorrelated with the distortion d (t), i.e.,

$$E\{s^*(t)d(t)\} = 0. \qquad (8)$$

and

$$\alpha_\gamma = \frac{E\{s^*(t)s_c(t)\}}{E\{s^*(t)s(t)\}} = E\{s^*(t)s_c(t)\}, \qquad (9)$$

due to the fact that E {|s(t)| 2} = 1. Note that when sc (t) is modeled as a non-stationary process, which is the case for the OFDM signal with PC, the time average (over the period of Ts) should be applied to (9) as it is still a function of t [24]. The SDR can be then defined as [25], [26]

$$\text{SDR} = \frac{E\{|\alpha_\gamma s(t)|^2\}}{E\{|d(t)|^2\}} = \frac{|\alpha_\gamma|^2}{P_{\text{av},d}}, \qquad (10)$$

Where P_{av}, d is the average power of the distortion component d(t).

We note that the above SDR expression is referred to as design SDR in [25], with the distortion power representing the sum of both in-band and out-of-band components. Since it does not require the knowledge of the second-order statistics of the signal (such as power spectrum density), it is amenable to mathematical analysis compared to the SDR evaluated for the in-band distortion only.

It is easy to observe from (5) and Fig. 1 that since p (t) depends on the random variables {ti} that represent the time instants of peaks, the basic properties of linear systems such as superposition and homogeneity may not be applicable. Furthermore, unlike CAF, because of its non-causality it cannot be modeled as a Hammerstein system (i.e., a memoryless nonlinearity followed by a linear function [27]). In what follows, based on the level-crossing theory of Gaussian processes, we demonstrate that theoretical derivation of approximate forms for αγ and P_{av}, d is possible.

A. Level-Crossing Rate Approximation of Peak Distribution

The generation of cancelling pulses depends on the event that the peaks higher than a given threshold occur. Therefore, the knowledge of the peak distribution of OFDM signals is necessary. However, as discussed in [2], even if we assume the baseband OFDM signal as a band-limited complex Gaussian process, the exact form of peak distribution is complicated and may not be expressed in a closed form. Nevertheless,

the level crossing rate of a Gaussian process can be represented in a closed form following the work of Rice [28]. For a strictly bandlimited OFDM signal, the average number of positive crossings of a given level r per OFDM symbol is expressed as [2, eq.(19)]

$$v_c^+(r) = \sqrt{\frac{\pi}{3}}\frac{N}{T_s} r e^{-r^2}. \qquad (11)$$

Furthermore, since the number of the level-crossings and that of the peaks tend to agree as the threshold r increases, the conditional probability that a peak ρ exceeds r given that it exceeds a reference level γ is expressed by [2, eq. (20)]

$$\Pr\{\rho > r | \rho > \gamma\} \approx \frac{v_c^+(r)}{v_c^+(\gamma)} = \frac{r e^{-r^2}}{\gamma e^{-\gamma^2}}, \quad r > \gamma > 1/\sqrt{2}. \qquad (12)$$

The conditional pdf of the peaks that exceed γ is then approximated as

$$f_\rho(r|\gamma) = \frac{d}{dr}\Pr\{\rho < r | \rho > \gamma\} \approx \frac{(2r^2-1)}{\gamma} e^{\gamma^2 - r^2}, \quad r > \gamma > 1/\sqrt{2}. \qquad (13)$$

Note that the above conditional pdf satisfies the condition

$$\int_\gamma^\infty f_\rho(r|\gamma)\, dr = 1, \qquad (14)$$

and thus is considered as a valid pdf over the range r > γ.

B. Attenuation Factor Expression Based on Peak Shape Approximation

Recall that for a given threshold γ, Nρ (γ) denotes the number of the peaks above γ during one OFDM symbol period. Conditioned that we observe Nρ (γ) peaks and by referring to (5), the cross-correlation term αγ in (9) can be calculated as

$$\alpha_\gamma = E\left\{s^*(t)s_c(t)\middle|N_\rho(\gamma)\right\} = E\left\{s^*(t)\left(s(t)-p(t)\right)\middle|N_\rho(\gamma)\right\} = 1 - \sum_{i=1}^{N_\rho(\gamma)} E\{s^*(t)p_i(t-t_i)\,|\,\rho_i > \gamma\}, \qquad (15)$$

Where we have applied the condition E{|s(t)| 2} = 1. Next, we assume that 1) the shape of the peak and that of the cancelling pulse match well within the two adjacent Nyquist intervals from the time instant of the peak and 2) the cancelling pulse is uncorrelated with s(t) elsewhere.

The first assumption allows us to express s(t) corresponding to the ith peak as

$$s(t) \approx \rho_i e^{j\theta_i} g(t-t_i), \quad t_i - T \le t \le t_i + T. \qquad (16)$$

Furthermore, by the second assumption the summand in the second term of (15) reduces to

$$E\left\{s^*(t)p_i(t-t_i)\ |\rho_i > \gamma\right\} = \begin{cases} E\{\rho_i(\rho_i-\gamma)\,|\rho_i > \gamma\}\,|g(\tau)|^2, & -T \le \tau \le T, \\ 0, & \text{otherwise}, \end{cases} \qquad (17)$$

Where τ = t − ti and thus αγ is guaranteed to have a real value. By defining

$$D(\tau;\gamma) = \begin{cases} \underbrace{E\{\rho(\rho-\gamma)\,|\rho > \gamma\}}_{C(\gamma)}, & -T \le \tau \le T, \\ 0, & \text{otherwise}, \end{cases} \qquad (18)$$

we may express (15) as

$$\alpha_\gamma = 1 - \sum_{i=1}^{N_\rho(\gamma)} D(\tau;\gamma)\,|g(\tau)|^2. \qquad (19)$$

The coefficient C(γ) defined in (18) corresponds to the distortion factor associated with each cancelling pulse, and it follows from (13) that

$$C(\gamma) = \int_{\gamma}^{\infty} r(r-\gamma) f_{\rho}(r|\gamma) \mathrm{d}r = \frac{\gamma + e^{\gamma^2}\sqrt{\pi}\,\mathrm{erfc}(\gamma)}{2\gamma}. \tag{20}$$

Note that even if γ is large, C(γ) cannot be zero. More specifically, we have

$$\lim_{\gamma \to \infty} C(\gamma) = \frac{1}{2}. \tag{21}$$

This is because we are evaluating the distortion conditioned that the peak exceeds a certain threshold γ , and this amount cannot be zero. Since the probability of having such a high peak itself approaches zero, this behavior can be justified.

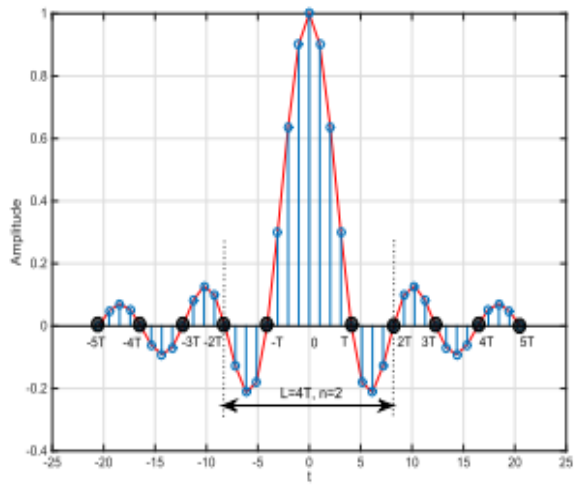

Fig.3. An example cancelling pulse kernel considered in this paper generated with the oversampling rate J = 4. The black dots indicate the special cases when n takes integer values.

C. Closed-Form Expression of Attenuation Factor

Considering the asymptote of N → ∞ and taking the time average, together with resorting to the strong law of large numbers, (19) can be simplified as

$$\alpha_{\gamma} \approx 1 - E\{N_{\rho}(\gamma)\} C(\gamma) \beta, \tag{22}$$

Where

$$\beta = \frac{1}{T_s} \int_{-T}^{T} |g(t)|^2 \, dt, \tag{23}$$

And

$$E\{N_p(\gamma)\} \approx v_c^{+}(\gamma) T_s = \sqrt{\frac{\pi}{3}} N \gamma e^{-\gamma^2}. \tag{24}$$

In this paper, we consider a band-limited OFDM signal that has a rectangular-like spectrum. Therefore, a sinc function with the same bandwidth can be used to approximate the cancelling pulse kernel, i.e.,

$$g(t) = w(t)\,\mathrm{sinc}(t/T), \quad -\infty < t < \infty, \tag{25}$$

Where w (t) is a window function and the sinc function is defined as

$$\mathrm{sinc}(x) = \frac{\sin(\pi x)}{\pi x}. \tag{26}$$

Various window functions can be applied, but without loss of generality, a rectangular function with length of L = 2nT is used in this paper:

$$w(t) = \begin{cases} 1, & -nT \le t \le nT, \\ 0, & \text{otherwise.} \end{cases} \quad (27)$$

In this work, we consider an oversampled OFDM signal for which the sampling period is denoted as T = T/J , where J is the oversampling rate. Note that in practice L should be a multiple of T , but n need not be an integer. Such a cancelling pulse kernel is depicted in Fig. 3, where it can be noticed that g(nT) = 0 when n is an integer.

Conditioned on the aforementioned sinc-like cancelling pulse, β defined in (23) can be calculated as

$$\beta = \frac{1}{T_s}\frac{2T}{\pi}\mathrm{Si}(2\pi) = \frac{2\mathrm{Si}(2\pi)}{\pi N}, \quad (28)$$

Where Si(·) is the sine integral, i.e.,

$$\mathrm{Si}(z) = \int_0^z \frac{\sin(t)}{t}\, dt, \quad (29)$$

and it follows that Si(2π) = 1.41815 .... As a result, an asymptote of αγ in the case of N → ∞ can be expressed in the following closed-form expression:

$$\alpha_\gamma \approx 1 - \frac{\mathrm{Si}(2\pi)}{\sqrt{3\pi}}\left\{\gamma e^{-\gamma^2} + \sqrt{\pi}\,\mathrm{erfc}(\gamma)\right\}. \quad (30)$$

D. Distortion Power Analysis based on Level-Crossing Rate Approximation

From (7), the average power of the distortion term Pav,d caused by PC can be written as

$$P_{\mathrm{av},d} = E\left\{|s_c(t)|^2 \,\middle|\, N_\rho(\gamma)\right\} - |\alpha_\gamma|^2, \quad (31)$$

Where the first term in the right hand side is the average power of the signal after PC with a proper time average operation and it can be further written as

$$\begin{aligned} E\left\{|s_c(t)|^2 \,\middle|\, N_\rho(\gamma)\right\} &= E\left\{|s(t) - p(t)|^2 \,\middle|\, N_\rho(\gamma)\right\} \\ &= E\left\{|p(t)|^2 \,\middle|\, N_\rho(\gamma)\right\} + 2\Re\{\alpha_\gamma\} - 1. \end{aligned} \quad (32)$$

Analogous to the derivation of (22), the first term in the right hand side of (32) can be expressed (after the time average over the period of Ts) as

$$\begin{aligned} E\left\{|p(t)|^2 \,\middle|\, N_\rho(\gamma)\right\} &= \sum_{i=1}^{N_\rho(\gamma)} E\left\{|p_i(t - t_i)|^2 \,\middle|\, N_\rho(\gamma)\right\} \\ &\approx E\left\{N_\rho(\gamma)\right\} B(\gamma)\eta, \end{aligned} \quad (33)$$

Where

$$\begin{aligned} B(\gamma) &= E\left\{(\rho - \gamma)^2 \,\middle|\, \rho > \gamma\right\} \\ &= \int_\gamma^\infty (r - \gamma)^2 f_\rho(r|\gamma)\mathrm{d}r \\ &= \frac{\sqrt{\pi}e^{\gamma^2}\mathrm{erfc}(\gamma)}{2\gamma} = C(\gamma) - \frac{1}{2}, \end{aligned} \quad (34)$$

and

$$\eta = \frac{1}{T_s}\int_{-\infty}^{\infty} |g(t)|^2\, \mathrm{d}t. \quad (35)$$

In the case that g(t) is given by (25), we have

$$\begin{aligned} \eta &= \frac{1}{T_s}\int_{-nT}^{nT} \mathrm{sinc}^2(t/T)\mathrm{d}t \\ &= \frac{1}{T_s}\frac{2T}{\pi}\mathrm{Si}(2n\pi) + \frac{1}{T_s}\frac{T(\cos(2n\pi) - 1)}{n\pi^2} \\ &= \frac{2}{N\pi}\mathrm{Si}(2n\pi) + \frac{\cos(2n\pi) - 1}{Nn\pi^2}. \end{aligned} \quad (36)$$

Collecting the above results and noticing that αγ has a real value, we obtain

$$P_{\mathrm{av},d} = \left(2\alpha_\gamma - 1 - |\alpha_\gamma|^2\right) + E\{N_\rho(\gamma)\}B(\gamma)\eta, \qquad (37)$$

and substituting αγ of (30) into (37) leads to the following closed-form expression:

$$P_{\mathrm{av},d} = \frac{\operatorname{erfc}(\gamma)\left(\mathrm{Si}(2n\pi) + \frac{(\cos(2n\pi)-1)}{2n\pi}\right)}{\sqrt{3}} - \frac{e^{-2\gamma^2}\left(\gamma + e^{\gamma^2}\sqrt{\pi}\operatorname{erfc}(\gamma)\right)^2 \mathrm{Si}(2\pi)^2}{3\pi}, \qquad (38)$$

Which indicates that the distortion term is dependent on the length of the window function n. Finally, substituting (30) and (38) into (10), the following closed-form expression of SDR can be obtained as a function of n and γ , i.e.,

$$\mathrm{SDR}(n,\gamma) = \frac{\left(\sqrt{3\pi} - \mathrm{Si}(2\pi)\left\{\gamma e^{-\gamma^2} + \sqrt{\pi}\operatorname{erfc}(\gamma)\right\}\right)^2}{\sqrt{3}\pi\operatorname{erfc}(\gamma)\mathrm{Si}(2n\pi) - e^{-2\gamma^2}\left(\gamma + e^{\gamma^2}\sqrt{\pi}\operatorname{erfc}(\gamma)\right)^2\mathrm{Si}(2\pi)^2}, \qquad (39)$$

for $n = 1, 2, \ldots$.

E. Remarks

In this work, we have chosen the sinc function as our cancelling pulse kernel for simplicity. Application of other functions is straightforward, but the derivation of SDR in a simple closed-form expression may not be necessarily guaranteed.

The two basic assumptions made here are the level-crossing approximation of peaks and the use of a sinc shape to approximate the peaks to be subtracted and without correlation outside the main lobe. The former assumption stems from the fact that the envelope threshold γ should be set relatively high in many practical applications of PC where the severe distortion is not tolerable from the viewpoint of out-of-band radiation. The latter one is introduced mainly to simplify the analysis such that the integration can be performed within the span of only the main lobe, rather than the entire length of the cancelling pulse kernel; it renders the subsequent mathematical analysis tractable.

IV. IN-BAND AND OUT-OF-BAND DISTORTION ANALYSIS

A finite-length property of a cancelling pulse kernel causes spurious in the signal power spectrum after PC. Since the adjacent power is generally subject to a regulatory constraint, an analysis of the out-of-band performance due to the use of PC plays an important role. In this section, we theoretically analyze the effect of the cancelling pulse on the ACLR. This also allows us to derive an EVM expression that takes into account only the in-band distortion.

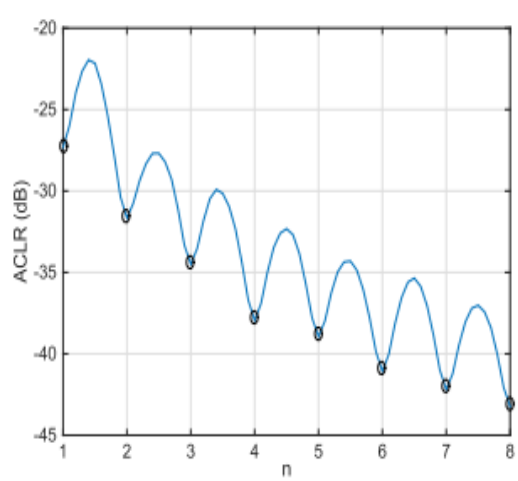

Fig.4. Relationship between the ACLR and the length n of a cancelling pulse kernel g(t); a sinc function is used as the cancelling pulse kernel.

A. Length of Cancelling Pulse Kernel

In our previous work on FPGA implementation of PC [10], it has been demonstrated that the length of the cancelling pulse kernel essentially leads to a trade-off between the out-of-band radiation and in-band distortion, and careful design is critical such that the resulting EVM and ACLR should meet the system requirement. More specifically, a longer cancelling pulse kernel can be used to achieve lower out-of-band level, but this not only increases implementation cost but also degrades the EVM performance. Therefore, a rigorous analysis of out-of-band distortion associated with the candidate cancelling pulse kernel is important.

For the cancelling pulse kernel g(t) defined in (25), its power spectrum density (PSD) Sg(f) can be calculated as

$$S_g(f) = \frac{T}{2N\pi^3}\left[\mathrm{Si}\left(n\pi\left(1-2Tf\right)\right)+\mathrm{Si}\left(n\pi\left(1+2Tf\right)\right)\right]^2. \tag{40}$$

Hence, the corresponding ACLR of g(t) can be expressed as

$$\zeta_g(n) = \frac{\int_{\mathcal{D}_{\text{out}}} S_g(f)\,df}{\int_{\mathcal{D}_{\text{in}}} S_g(f)\,df}, \tag{41}$$

Where D_{in} and D_{out} represent the frequency regions corresponding to in-band and adjacent channel, respectively. In Fig. 4, (41) is plotted for Sg (f) of (40) as a function of n, where Dout is defined later in Fig. 5. It is observed that minimum values of ACLR can be achieved for an integer value of n, i.e., when L is a multiple of T . Hence, we only focus on the cases where n takes an integer value in what follows. It thus follows that the larger value of n leads to better ACLR but at the cost of increasing in-band distortion, since both (41) and (39) monotonically decrease with increasing integer values of n.

B. ACLR Analysis

The previous subsection has shown that larger n generally leads to lower out-of-band emission, but it also results in severer in-band distortion with higher hardware overhead. Moreover, as the occurrence of the peaks higher than the threshold becomes a rare event, the out-of-band power added to the original signal should be relatively low. Consequently, the integer n need not be necessarily very large to meet the spectral requirement. If we assume that the original signal has sufficiently low out of-band level, the ACLR of the PC output signal is determined exclusively by the cancelling pulses that are added to the input signal. Nevertheless, since the amplitude of each cancelling pulse kernel is adjusted to the observed peak level, the out-of band power caused by the cancelling pulses is related to the statistical distribution of the peaks.

In this paper, the average (long term) PSD of the peak cancelled signal is considered for the evaluation of ACLR. Observing that 1) each cancelling pulse pi(t) becomes zero or has negligibly small value as |t| increases and 2) the two distinct cancelling pulses pi(t − ti) and p j(t − tj) are likely to have temporal separation as the threshold γ increases, it may be reasonable to assume that the cross correlation among the peak cancelling pulses are negligible.

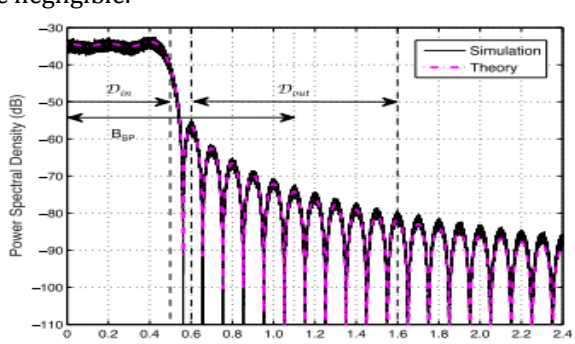

Fig.5. Averaged PSD of the cancelling pulses with n = 5, γ = 4dB, and J = 8, where Din and Dout are the regions of occupied and adjacent channels, respectively, and BSP denotes the channel spacing between them. The bandwidth is normalized by the inverse of the Nyquist interval, i.e., 1/T , which is equivalent to the bandwidth of the in-band OFDM signal.

Therefore, the autocorrelation function of p(t) defined in (5) may be expressed as

$$R_p(\tau) = \sum_{i=1}^{N_\rho(\gamma)} R_{p_i}(\tau), \qquad (42)$$

Where Rpi (τ) is the autocorrelation of pi(t) averaged over the time period Ts and is given by

$$R_{p_i}(\tau) = \frac{1}{T_s}\int_0^{T_s} E\left\{p_i^*(t+\tau)p_i(t)\right\} dt$$
$$= E\left\{(\rho_i - \gamma)^2\right\} \frac{1}{T_s}\int_0^{T_s} g^*(t+\tau)g(t)dt. \qquad (43)$$

Therefore, we can obtain its PSD by Fourier transform of (43) with Ts → ∞ as

$$P_{p_i}(f) = E\left\{(\rho_i - \gamma)^2\right\} S_g(f), \qquad (44)$$

where Sg(f) denotes the PSD of g(t) derived in (40). Finally, invoking the strong law of large numbers, the PSD of p(t) can be written as

$$P_p(f) = \sum_{i=1}^{N_\rho(\gamma)} P_{p_i}(f) \approx E\{N_\rho(\gamma)\}B(\gamma)S_g(f)$$
$$= \frac{T\,\mathrm{erfc}(\gamma)}{4\sqrt{3}\pi^2}\left[\mathrm{Si}(n\pi(1-2Tf)) + \mathrm{Si}(n\pi(1+2Tf))\right]^2, \qquad (45)$$

Where B (γ) is previously defined in (34). To show the validity of (45), the approximated PSD and its simulation results are plotted in Fig. 5, where the length of cancelling pulse is set to n = 5, the target PAPR γ is 4 dB, and the oversampling rate J is 8. The bandwidths of Din and Dout are denoted by Bin and Bout, respectively, and in this example we assume Bin = Bout = 1. As is observed from Fig. 5, we can see that (45) can accurately predict the PSD of the cancelling pulses. As previously mentioned, we assume that the original signal has PSD with negligible out-of-band power. Consequently, the cancelling pulse is the only source of the out-of-band power. The in-band power of the PC output, on the other hand, can be seen as the summation of both in-band signal and its uncorrelated in-band distortion component. Let Ps(f), Psc (f), and Pd (f) denote the PSDs of the input signal s(t), the output signal with PC sc(t), and the resulting distortion component d(t), respectively. Similar to (41), the ACLR for the output signal with PC, denoted by ζSc (n,γ), becomes

$$\zeta_{S_c}(n,\gamma) = \frac{\int_{\mathcal{D}_{\text{out}}} P_{s_c}(f)df}{\int_{\mathcal{D}_{\text{in}}} P_{s_c}(f)df}$$
$$= \frac{\int_{\mathcal{D}_{\text{out}}} P_p(f)df}{\alpha_\gamma^2\int_{\mathcal{D}_{\text{in}}} P_s(f)df + \int_{\mathcal{D}_{\text{in}}} P_d(f)df}. \qquad (46)$$

Therefore, our remaining task is to find Pd (f). Combining (7) and (5), an alternative expression of p(t) is given by

$$p(t) = \left(1-\alpha_\gamma\right)s(t) - d(t). \qquad (47)$$

Considering the fact that s(t) and d(t) are uncorrelated, we further have

$$P_d(f) = P_p(f) - \left(1-\alpha_\gamma\right)^2 P_s(f), \quad f \in \mathcal{D}_{\text{in}}. \qquad (48)$$

Hence, (46) reduces to

$$\zeta_{S_c}(n,\gamma) = \frac{\int_{\mathcal{D}_{\text{out}}} P_p(f)df}{\int_{\mathcal{D}_{\text{in}}} P_p(f)\,df - \left(1-2\alpha_\gamma\right)\int_{\mathcal{D}_{\text{in}}} P_s(f)\,df}. \qquad (49)$$

With the Parseval's $\int_{\mathcal{D}_{\text{in}}} P_s(f)\,df = E\{|s(t)|^2\} = 1$, (49) can be further simplified as

$$\zeta_{S_c}(n,\gamma)=\frac{\int_{\mathcal{D}_{\text{out}}}P_p(f)df}{\int_{\mathcal{D}_{\text{in}}}P_p(f)\,df-(1-2\alpha_\gamma)}. \qquad (50)$$

By observing (45), it can be concluded that the ACLR of (50) depends on n, i.e., the window size of g(t) as well as γ as expected. The accuracy of the derived results will be numerically evaluated in Section V. C. EVM Analysis In wireless transceivers, EVM is a commonly adopted measure of the in-band distortion. It can be approximated by the effective SDR as [25]

$$\text{EVM}=\sqrt{\frac{1}{\text{SDR}_{\text{eff}}}}\times 100\%. \qquad (51)$$

The effective SDR denoted by SDR_{eff} is the power ratio of the attenuated signal and its in-band distortion, which can be expressed as

$$\text{SDR}_{\text{eff}}=\frac{\alpha_\gamma^2\int_{\mathcal{D}_{\text{in}}}P_s(f)df}{\int_{\mathcal{D}_{\text{in}}}P_d(f)df}=\frac{\alpha_\gamma^2\int_{\mathcal{D}_{\text{in}}}P_s(f)df}{\int_{\mathcal{D}_{\text{in}}}\left[P_p(f)-(1-\alpha_\gamma)^2P_s(f)\right]df}. \qquad (52)$$

Hence, the EVM of the PC output can be written as

$$\text{EVM}=\frac{1}{\alpha_\gamma}\sqrt{\int_{D_{\text{in}}}P_p(f)\,df-(1-\alpha_\gamma)^2}\times 100\%, \qquad (53)$$

based on the fact that D_{in} Ps (f) d f = 1.

C. SER Over an AWGN Channel

In the rest of this section, we analyze the SER when the PAPR reduced signal is transmitted over an AWGN channel. In order to investigate the effect of PC, we only consider the SER without channel coding. As PC is applied to the OFDM symbols that have the peaks exceeding the threshold, the received signal corresponding to (7) can be expressed as

$$s_o(t)=\begin{cases}\alpha s(t)+d(t)+n(t), & \text{when PC is applied,}\\ s(t)+n(t), & \text{otherwise,}\end{cases} \qquad (54)$$

Where n(t) is an AWGN term with its variance denoted by $P_{av,n}$. With the effect of additional white noise, it is reasonable to decompose the input signal into the following two cases: In the case that PC is applied, since the distortion and the channel noise are statistically independent, signal-to-noise plus-distortion ratio (SNDR) should be taken into consideration and thus we use Pe (SNDR) to represent the error probability. In the other case, Pe (SNR) is used to describe the error.

Thus, similar to the analysis in [29], the average SER Pe, total is expressed as

$$P_{e,\text{total}}=\Gamma_C(\gamma)\cdot P_e(\text{SNDR})+(1-\Gamma_C(\gamma))\cdot P_e(\text{SNR}), \qquad (55)$$

With C (γ) representing the complementary cumulative distribution function (CCDF) of the PAPR for the band-limited OFDM signals. A closed-form approximation of C (γ) can be found in [2]. The evaluation of the above error probability requires the knowledge of pdf of d(t), and it has been commonly assumed that d(t) approaches complex Gaussian distribution having zero mean and variance of Pav,d as the number of subcarriers N increases [14], [15]. Due to the assumption that the original signal component and distortion are not correlated in frequency domain, the distortion component can be regarded as an additional noise. Accordingly, the effective (in-band) SNDR which incorporates both channel noise and distortion can be written as

$$\text{SNDR}=\frac{\alpha_\gamma^2E\{|s(t)|^2\}}{P_{\text{av},n}+\int_{\mathcal{D}_{\text{in}}}P_d(f)\,df}. \qquad (56)$$

In a similar manner, SNR for the second case is given by

$$\mathrm{SNR} = \frac{E\left\{|s(t)|^2\right\}}{P_{\mathrm{av},n}}. \qquad (57)$$

It should be noted that the equivalent average in-band signal power to be transmitted is denoted by (1 – C(γ)) + C(γ)α2 γ . Under these assumptions, for an ideal receiver with perfect synchronization, the SER can be evaluated as a general function of modulation order M and SNR:

$$P_e(\mathrm{SNR}) = f(M, \mathrm{SNR}). \qquad (58)$$

In this paper, considering an M-ary rectangular quadrature amplitude modulated (M-QAM) baseband signal, we have [21]

$$f(M, \mathrm{SNR}) = 4\left(1 - \frac{1}{\sqrt{M}}\right) Q\left(\sqrt{\frac{3\log_2(M)}{M-1}\mathrm{SNR}}\right) \times \left(1 - \left(1 - \frac{1}{\sqrt{M}}\right) Q\left(\sqrt{\frac{3\log_2(M)}{M-1}\mathrm{SNR}}\right)\right). \qquad (59)$$

Where

$$Q(x) = (1/2)\mathrm{erfc}(x/\sqrt{2}) = (1/\sqrt{2\pi})\int_x^{\infty} e^{-t^2/2}dt.$$

When PC distortion is imposed, the SNR in f (M, SNR) should be replaced by SNDR.

V. NUMERICAL RESULTS

The accuracies of the theoretical expressions derived in the previous sections are evaluated by computer simulations. The OFDM symbol is generated with all the subcarriers modulated by 16-QAM. In order to acquire accurate peak positions for PC, the OFDM symbol is oversampled by J = 8 times. The cancelling pulse is a sinc function, with a length of 80 samples, i.e., L = 80 T and thus n = L/2T = L/(2J T) = 5, which is chosen to ensure an acceptable ACLR.

We begin with the investigation of the attenuation factor αγ with respect to the target PAPR γ , which is reported in Fig. 6. For the purpose of demonstrating the convergence behavior of simulation results, the number of subcarriers is set to 500, 1000, 5000, and 10000. It is observed that the theoretical attenuation factor αγ serves as an asymptote for the OFDM system with a large number of subcarriers.

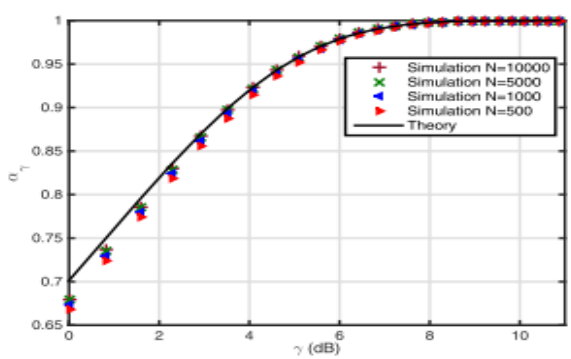

Fig.6. Performance of attenuation factor αγ with respect to different target PAPR γ.

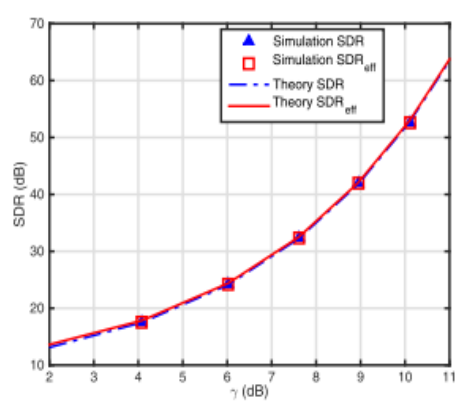

Fig.7. SDRs with respect to different target PAPR γ.

Furthermore, in high γ region, the theoretical curve well agrees with all the simulated results as expected. In practice, one may be interested only in the cases with γ > 6dB, as the threshold lower than this would result in unacceptable amount of distortion. We choose N = 10000 for all the subsequent simulation results.

In Fig. 7, both the theoretical and simulated SDRs under different threshold levels are plotted. The theoretical results match well with the simulation result, which shows that our analysis provides good fidelity for predicting the amount of distortion. In the figure, SDReff refers to the effective SDR, which is a metric that takes into account only the in-band distortion imposed on the desired signal. Due to the fact that a practical PC design introduces low out-of-band distortion, the gap between SDReff and SDR is negligible.

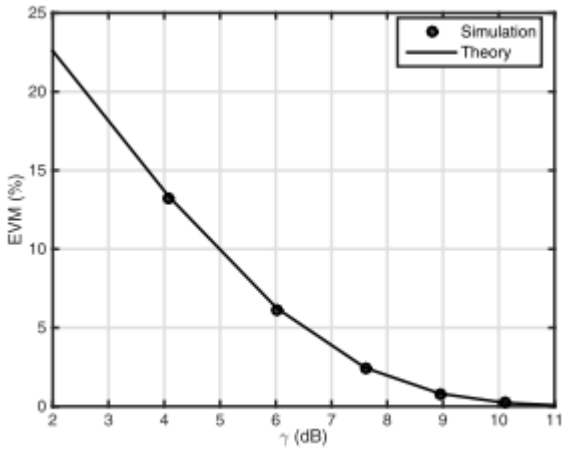

Fig.8.Simulated and theoretical EVM with respect to different target PAPR γ.

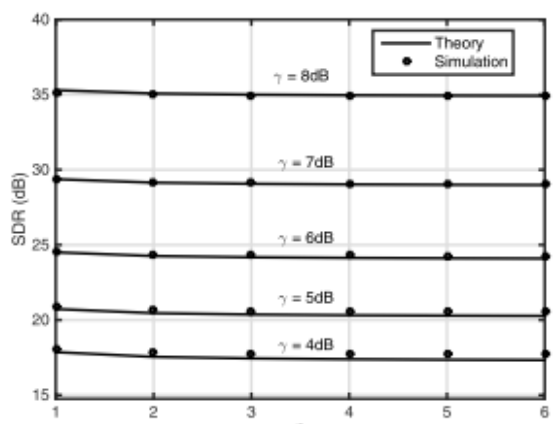

Fig.9. SDR with respect to the length of cancelling pulse n under different target PAPR γ.

In order to demonstrate the effectiveness of our approximation of the in-band distortion, Fig. 8 shows the EVM performance in conjunction with its analytical expression given in (53). A good agreement between the theoretical and simulation results is observed.

The effect of cancelling pulse length n on SDR, where n is chosen from integer values, is compared in Fig. 9. This result elucidates the fact that SDR is dominated by the threshold value γ , which agrees with the SDR result shown in Fig. 7. We also observe that smaller cancelling pulse length n results in better SDR, but its effect is negligible when n > 3. This is due to fact that the side lobe of the cancelling pulse vanishes rapidly with increasing n.

Similarly, the ACLRs in terms of n are illustrated in Fig. 10, where the width of channel spacing BSP defined in Fig. 5 is set to 1.1Bin in order to reserve a small guard band between the occupied channel and adjacent channel. From Fig. 10, it is observed that the analytical results can serve as a good approximation of the simulated ACLRs. The gaps between different ACLR curves become larger when the threshold γ is increased. The ACLR decreases with the increasing pulse length n due to reduced discontinuity between the head and the tail of cancelling pulse kernel. Unlike the effect on SDR shown in Fig. 9,

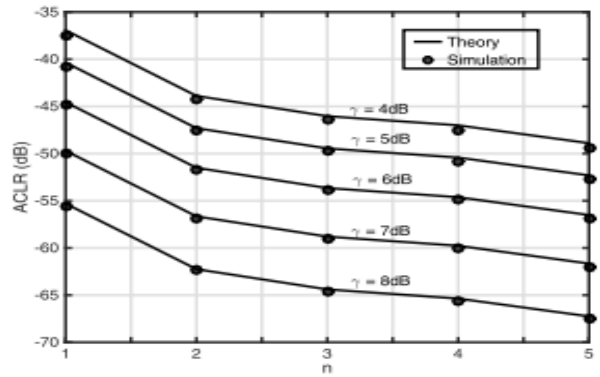

Fig.10. ACLRs with respect to different pulse length n under different target PAPR γ.

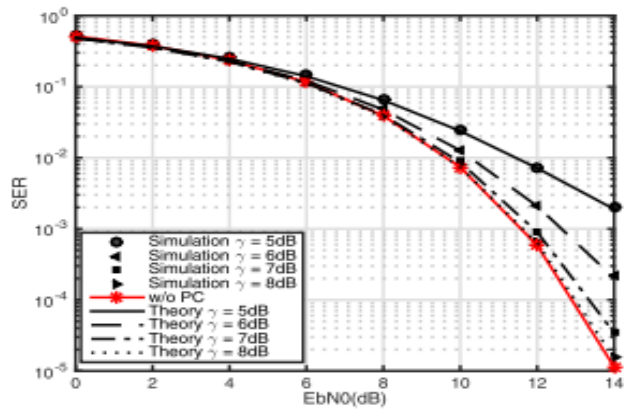

Fig.11. SER over an AWGN channel with respect to different target PAPR γ of 16-QAM OFDM signals in the presence of PC.

both the pulse length n and the threshold γ have a significant impact on the ACLR. Given the results observed from Fig. 9 and Fig. 10, it can be concluded that n and γ should be appropriately chosen according to the spectral mask as well as the distortion requirement and our theoretical analysis serves as a guideline in determining these values.

We now turn to the SER performance over an AWGN channel in the presence of PC. The simulated SER plots for different noise levels with various threshold values γ (5 dB, 6 dB, 7 dB, and 8 dB) are shown in Fig. 11, along with the theoretical approximation. It can be observed that in the higher SNR region where the effect of nonlinear distortion caused by PC becomes apparent, good agreement between theoretical analysis and simulation results can be observed.

RESULTS

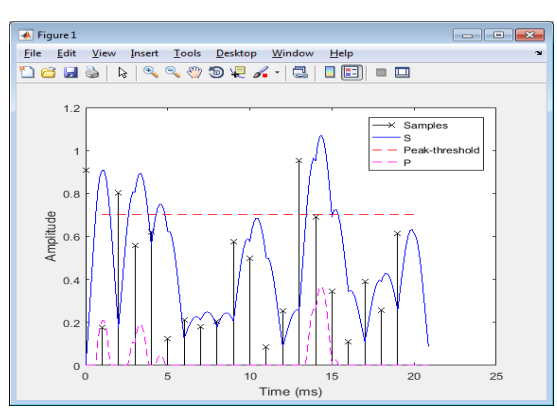

Fig.1. Example waveforms associated with PC where ρi denotes the envelope level of the ith peak.

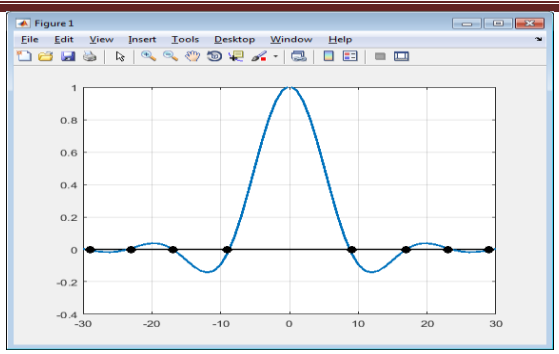

Fig.2. An example cancelling pulse kernel considered in this paper generated with the oversampling rate J = 4. The black dots indicate the special cases when n takes integer values.

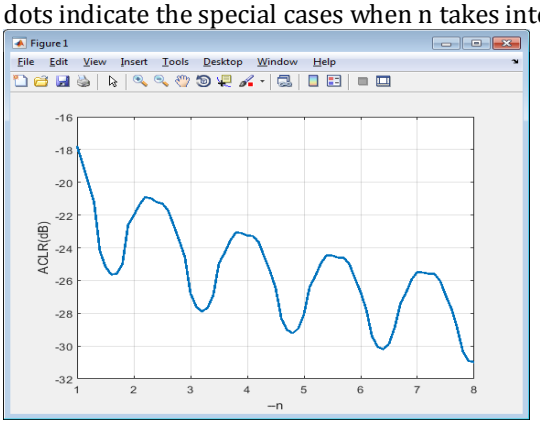

Fig.3. Relationship between the ACLR and the length n of a cancelling pulse kernel g(t); a sinc function is used as the cancelling pulse kernel.

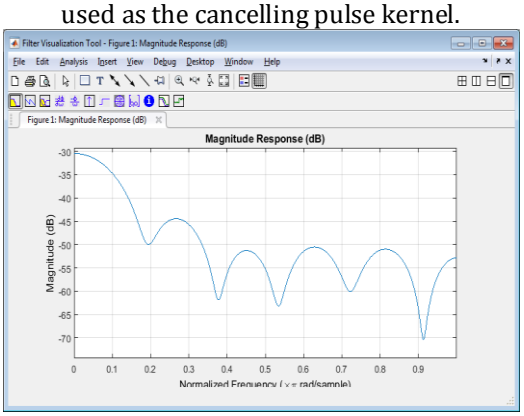

Fig.4. Averaged PSD of the cancelling pulses with n = 5, γ = 4dB, and J = 8, where Din and Dout are the regions of occupied and adjacent channels, respectively, and BSP denotes the channel spacing between them. The bandwidth is normalized by the inverse of the Nyquist interval, i.e., 1/T , which is equivalent to the bandwidth of the in-band OFDM signal.

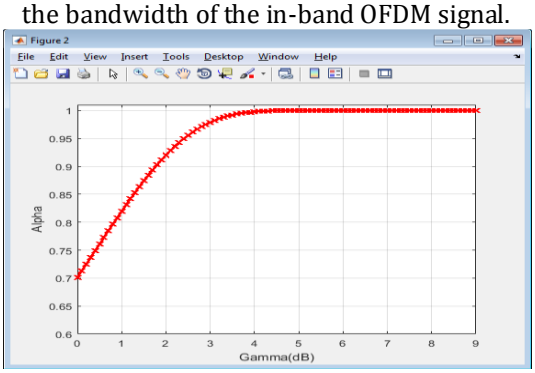

Fig.5. Performance of attenuation factor αγ with respect to different target PAPR γ.

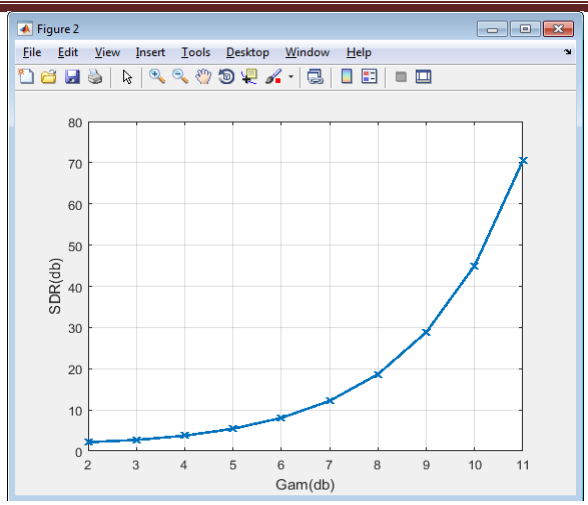

Fig.6. SDRs with respect to different target PAPR γ.

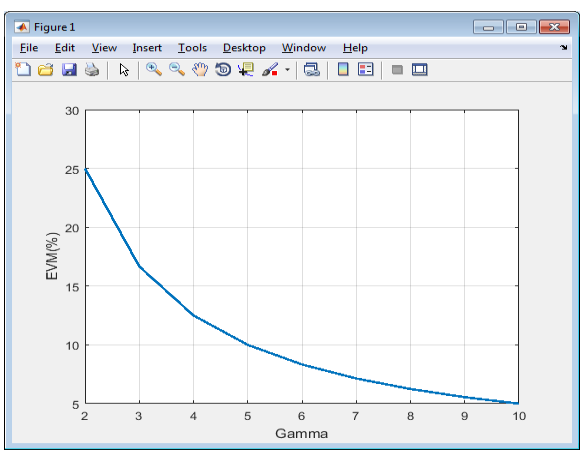

Fig.7.Simulated and theoretical EVM with respect to different target PAPR γ.

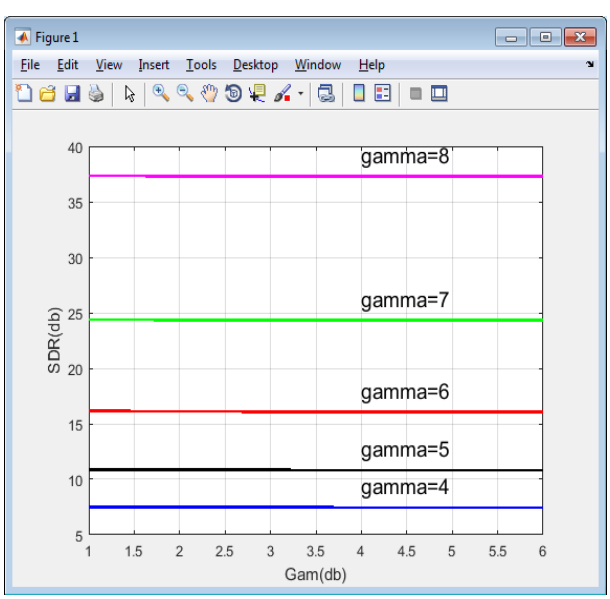

Fig.8. SDR with respect to the length of cancelling pulse n under different target PAPR γ.

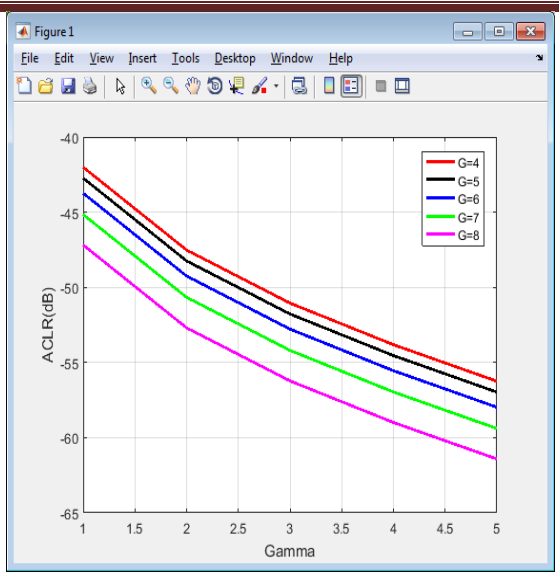

Fig.9. ACLRs with respect to different pulse length n under different target PAPR γ.

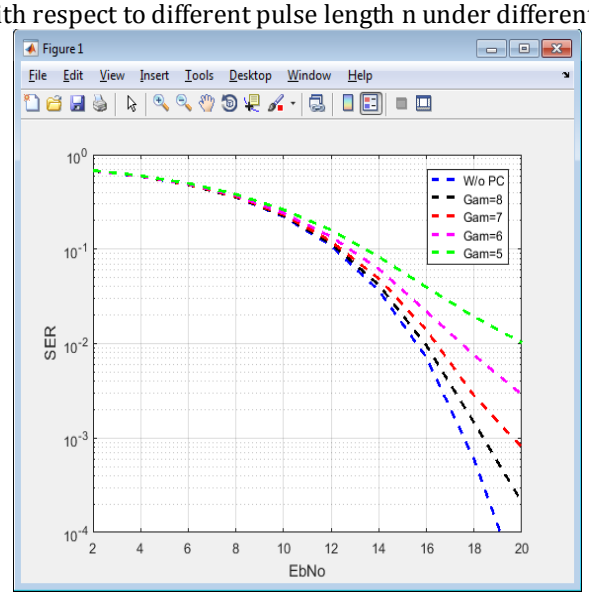

Fig.10. SER over an AWGN channel with respect to different target PAPR γ of 16-QAM OFDM signals in the presence of PC.

VI. CONCLUSION

In this paper, theoretical analysis of both in-band and out-of band distortion performance of peak cancellation is carried out for OFDM systems. The closed-form expression of SDR caused by PC is first obtained, with which the effect of PC in terms of EVM and ACLR associated with the peak reduced signal is analyzed from the frequency domain perspective.

In addition, the resulting SER degradation caused by PC when transmitted over an AWGN channel is mathematically formulated. The effectiveness of the analytical approach given in this paper is well confirmed by simulation results. The analytical tools developed in this work serve as a useful guideline for designing cancelling pulses of PC-based OFDM systems. They can be also used for estimating its effectiveness as well as limitations in view of system requirements.

REFERENCES

1. S. Bahai and B. R. Saltzberg, Multicarrier Digital Communications: Theory and Applications of OFDM, Kluwer Academic, 1999.
2. P. S. Chow, J.M. Cioffi, J. A. C. Bingham, "A practical discrete multitone transceiver loading algorithm for data transmission over spectrally shaped channels," IEEE Trans. Commun., vol. 43, no. 2, pp. 773 -775, Feb.-March-April 1995.

3. H. Rohling et al., "Broadband OFDM radio transmission for multimedia applications," Proc. IEEE, vol. 87, no. 10, pp. 1778- 1789, Oct. 1999.
4. X. Li and L. J. Cimini, "Effects of clipping and filtering on the performance of OFDM," IEEE VTC '97, pp. 1634-1638.
5. H. Ochiai and H. Imai, "On the distribution of the peak-to average power ratio in OFDM signals," IEEE Trans. Commun., vol. 49, pp.282-289 , Feb. 2001.
6. T. Hentschel, M. Henker, and G. Fettweis, "The digital front-end of software radio terminals," IEEE Pers. Commun., vol. 6, no. 4, pp. 40–46, Aug. 1999.
7. ETSI 3rd Generation Partnership Project (3GPP), "User equipment (UE) radio transmission and reception," The European Telecommunications Standards Inst., Sophia-Antipolis, France, TS 136.101, Jun. 2011.
8. R. Bauml, R. F. H. Fischer, and J. Huber, "Reducing the peak-to-average power ratio of multicarrier modulation by selected mapping," Electron. Lett., vol. 32, no. 22, pp. 2056–2057, Oct. 1996.
9. H. Ochiai and H. Imai, "Performance analysis of deliberately clipped OFDM signals," IEEE Trans. Commun., vol. 50, no. 1, pp. 89–101, Jan. 2002.
10. X. Li and L. J. Cimini, "Effects of clipping and filtering on the performance of OFDM," in Proc. IEEE Veh. Technol. Conf. (VTC'97), May 1997, vol. 3, pp. 1634–1638.
11. T. May and H. Rohling, "Reducing the peak-to-average power ratio in OFDM radio transmission systems," in Proc. IEEE Veh. Technol. Conf. (VTC'98), May 1998, vol. 3, pp. 2474–2478.
12. J. Song and H. Ochiai, "FPGA implementation of peak cancellation for PAPR reduction of OFDM signals," in Proc. IEEE Int. Conf. Commun. Syst. (ICCS'14), pp. 414–418, Nov. 2014.
13. J. Song and H. Ochiai, "A low-complexity peak cancellation scheme and its FPGA implementation for peak-to-average power ratio reduction," EURASIP J. Wireless Commun. Netw. vol. 2015, pp. 1–14, Mar. 2015.
14. H. B. Jeon, J. S. No, and D. J. Shin, "A new PAPR reduction scheme using efficient peak cancellation for OFDM systems," IEEE Trans. Broadcast., vol. 58, no. 4, pp. 619–628, Dec. 2012.
15. L. Wang and C. Tellambura, "Analysis of clipping noise and Tone Reservation algorithms for peak reduction in OFDM systems," IEEE Trans. Veh. Technol., vol. 57, no. 3, pp. 1675–1694, May 2008.
16. H. Ochiai and H. Imai, "Performance of the deliberate clipping with adaptive symbol selection for strictly band-limited OFDM systems," IEEE J. Sel. Areas Commun., vol. 18, no. 11, pp. 2270–2277, Nov. 2000.
17. R. Dinis and A. Gusmao, "A class of nonlinear signal-processing schemes for bandwidth-efficient OFDM transmission with low envelope fluctuation," IEEE Trans. Commun., vol. 52, no. 10, pp. 2009–2018, Oct. 2004.
18. Dardari, V. Tralli, and A. Vaccari, "A theoretical characterization of nonlinear distortion effects in OFDM systems," IEEE Trans. Commun., vol. 48, no. 10, pp. 1755–1764, Oct. 2000.
19. Costa and S. Pupolin, "M-QAM-OFDM system performance in the presence of a nonlinear amplifier and phase noise," IEEE Trans. Commun., vol. 50, no. 3, pp. 462–472, Mar. 2002.
20. Y. Xiao, W. Bai, L. Dan, G. Wu, and S. Li, "Performance analysis of peak cancellation in OFDM systems," Sci. China Inf. Sci., vol. 55, pp. 789– 794, Apr. 2012.
21. R. Price, "A useful theorem for nonlinear devices having gaussian inputs," IRE Trans. Inf. Theory, vol. 4, no. 2, pp. 69–72, Jun. 1958.
22. J. J. Bussgang, "Crosscorrelation functions of amplitude-distorted Gaussian signals," Res. Lab. Electron., Massachusetts Inst. Technol., Cambridge, MA, USA, Tech. Rep. 216, Mar. 1952.
23. H. Rowe, "Memoryless nonlinearities with Gaussian inputs: Elementary results," Bell Syst. Tech. J., vol. 61, pp. 1519–1526, Sep. 1982.
24. J. G. Proakis and M. Salehi, Digital Communications, 5th ed. New York, NY, USA: McGraw-Hill, 2008.
25. H. Ochiai, "An analysis of band-limited communication systems from amplifier efficiency and distortion perspective," IEEE Trans. Commun., vol. 61, no. 4, pp. 1460–1472, Feb. 2013.
26. P. Banelli and S. Cacopardi, "Theoretical analysis and performance of OFDM signals in nonlinear AWGN channels," IEEE Trans. Commun., vol. 48, no. 3, pp. 430–441, Mar. 2000.
27. Y. Kibangou and G. Favier, "Wiener-Hammerstein systems modeling using diagonal Volterra kernels coefficients," IEEE Signal Process. Lett., vol. 13, no. 6, p. 381, Jun. 2006.
28. S. O. Rice, "Mathematical analysis of random noise," Bell Syst. Tech. J., vol. 23, pp. 282–332, Jul. 1944.
29. R. Bahai, M. Singh, A. J. Goldsmith, and B. R. Saltzberg, "A new approach for evaluating clipping distortion in multicarrier systems," IEEE J. Sel. Areas Commun., vol. 20, no. 5, pp. 1037–1046, Jun. 2002